Supporting information for: SAXS-restrained ensemble simulations of intrinsically disordered proteins with commitment to the principle of maximum entropy

Markus R. Hermann[†] and Jochen S. Hub[*,‡]

[†]*Institute for Microbiology and Genetics, Georg-August-Universität Göttingen, Göttingen, Germany*

[‡]*Theoretical Physics and Center for Biophysics, Saarland University, Campus E2 6, 66123 Saarbrücken, Germany*

E-mail: jochen.hub@uni-saarland.de

Supporting Information Figures

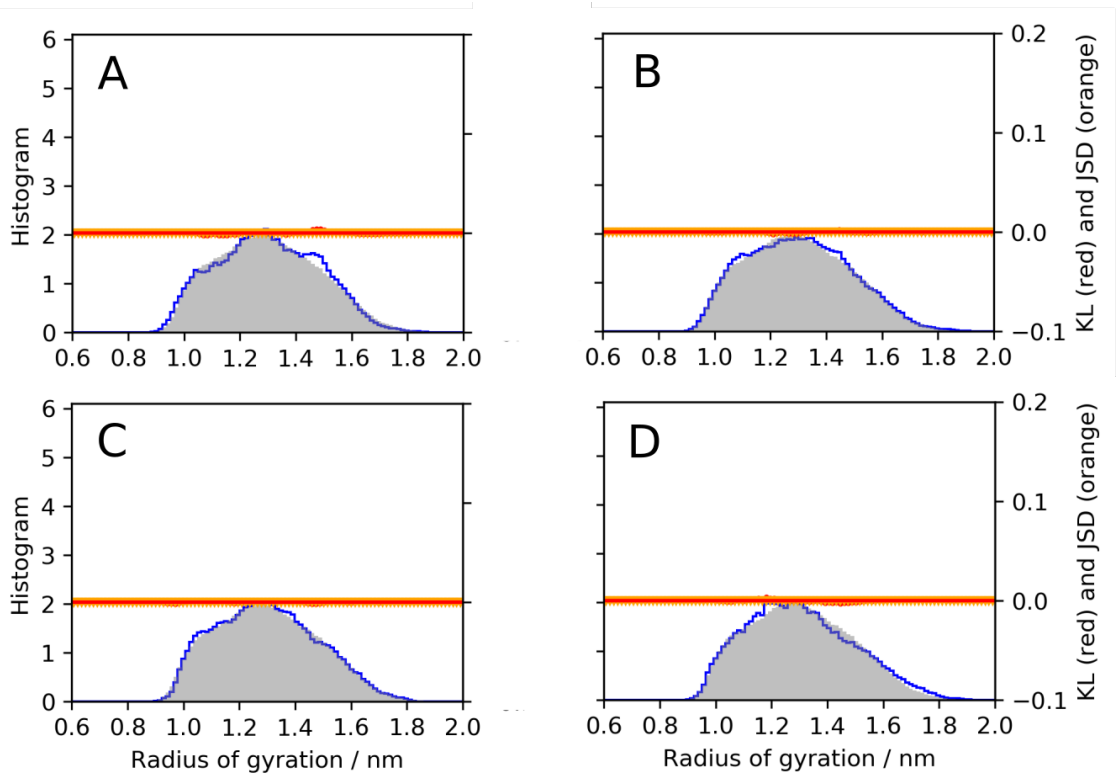

Figure S1: Binning analysis of the distribution of the radius of gyration R_g taken from the SAXS-restrained simulation with Amber99SBws/TIP3P using 4 replicas, coupled to experimental SAXS data. The grey distribution was computed from the complete 400 ns simulation, omitting the first 2 ns for equilibration. Blue curves show the R_g distribution computed from the following time bins: (A) 2–100 ns, (B) 100–200 ns, (C) 200–300 ns, (D) 300–400 ns. The agreement between the R_g distributions from different time bins (A–D) suggests that the ensemble is reasonably converged.

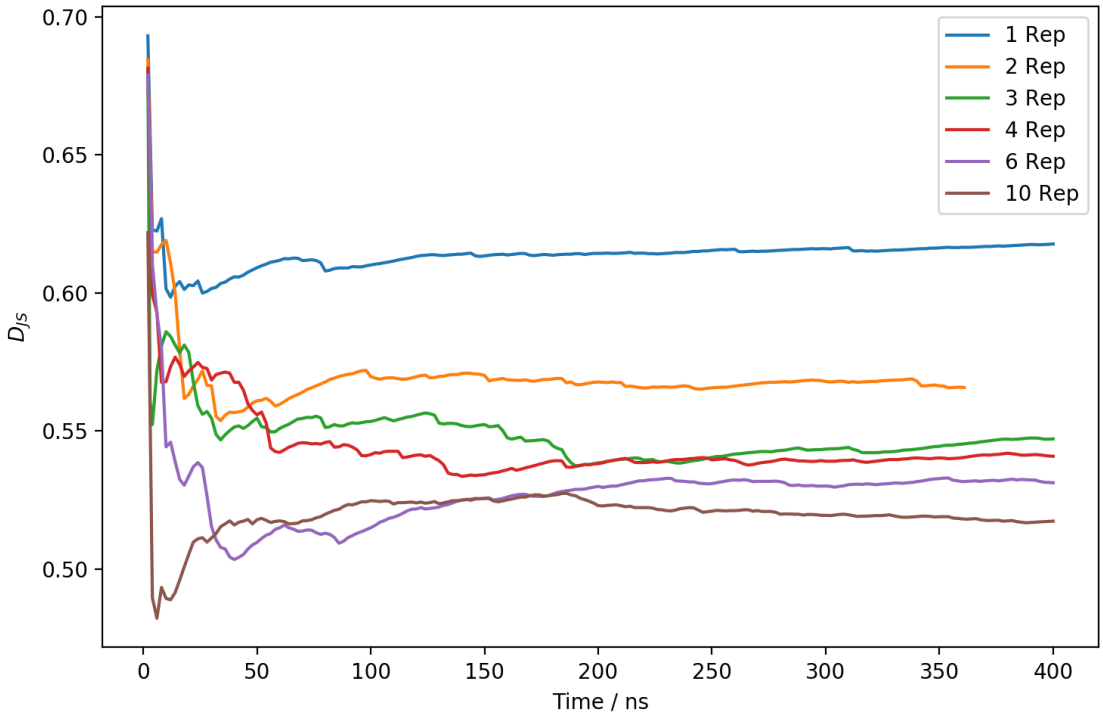

Figure S2: Convergence of the Jensen–Shannon divergence D_{JS} with simulation time. The abscissa shows simulation time per replica. The colors refer to different numbers of replicas (see legend). Total simulation time is given by multiplication with the number of replicas. The analysis confirms that, after 400 ns (360 ns for the two-replica simulation), D_{JS} is reasonably converged.

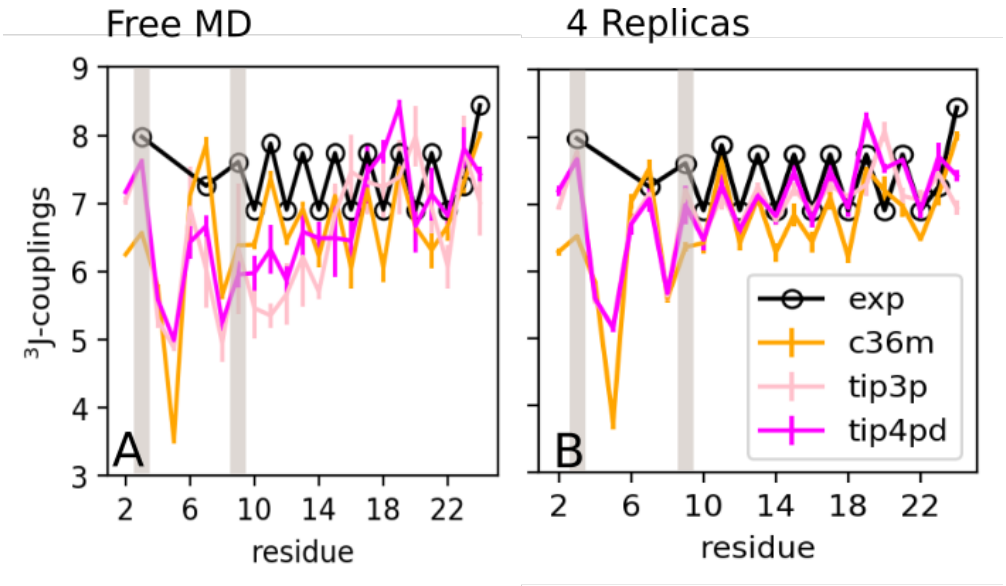

Figure S3: Comparison of $^3J_{\mathrm{HN\text{-}H\alpha}}$-couplings between experiment (black) and simulations conducted with three force fields (colored curves, see legend). Evidently, differences between the force fields found in free MD simulation (A) are greatly reduced in ensemble-restraint simulations using four replicas (B), except for the N-terminal region with residue numbers $\leq$5. Shaded vertical bars indicate residues 3 and 9 whose ϕ angle distributions are shown in Figs. S4 and S5

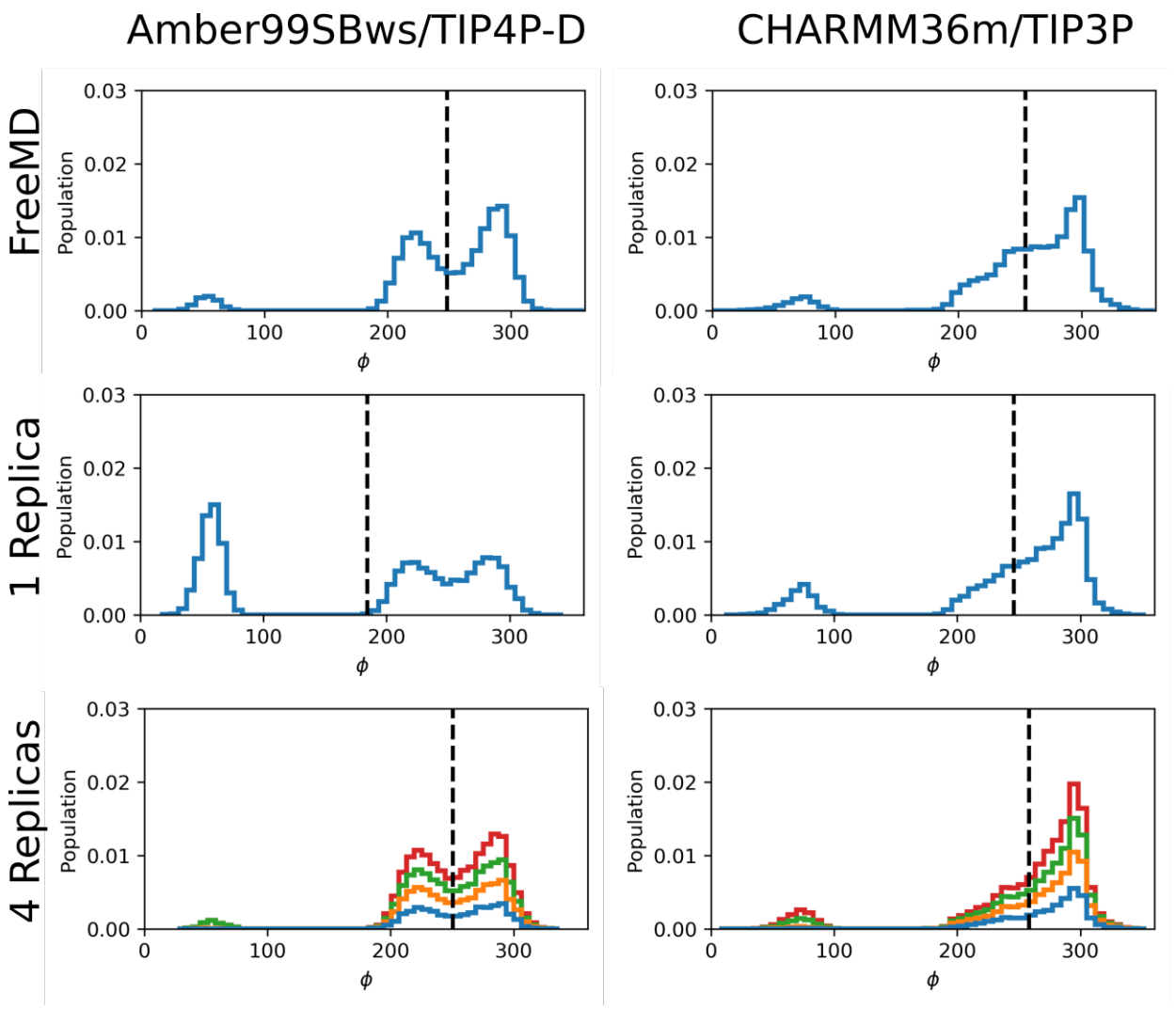

Figure S4: Distributions of the dihedral angle ϕ of residue 3 for Amber99SBws/TIP4P-D (left column) and CHARMM36m (right column). Top row: free MD; middle row: single-replica refinement; bottom row: four-replica refinement. Two findings are noteworthy: (i) For Amber99SBws/TIP4P-D, single-replica refinement led to a spuriously overpopulated angle at $\phi \approx 60°$ (left middle plot). (ii) The differences between Amber99SBws/TIP4P-D and CHARMM36m are not mitigated by refinement to SAXS data (compare top with bottom row), in line with different $^3J_{\text{HN-H}\alpha}$-couplings at residue 3 (Fig. S3, shaded vertical bars).

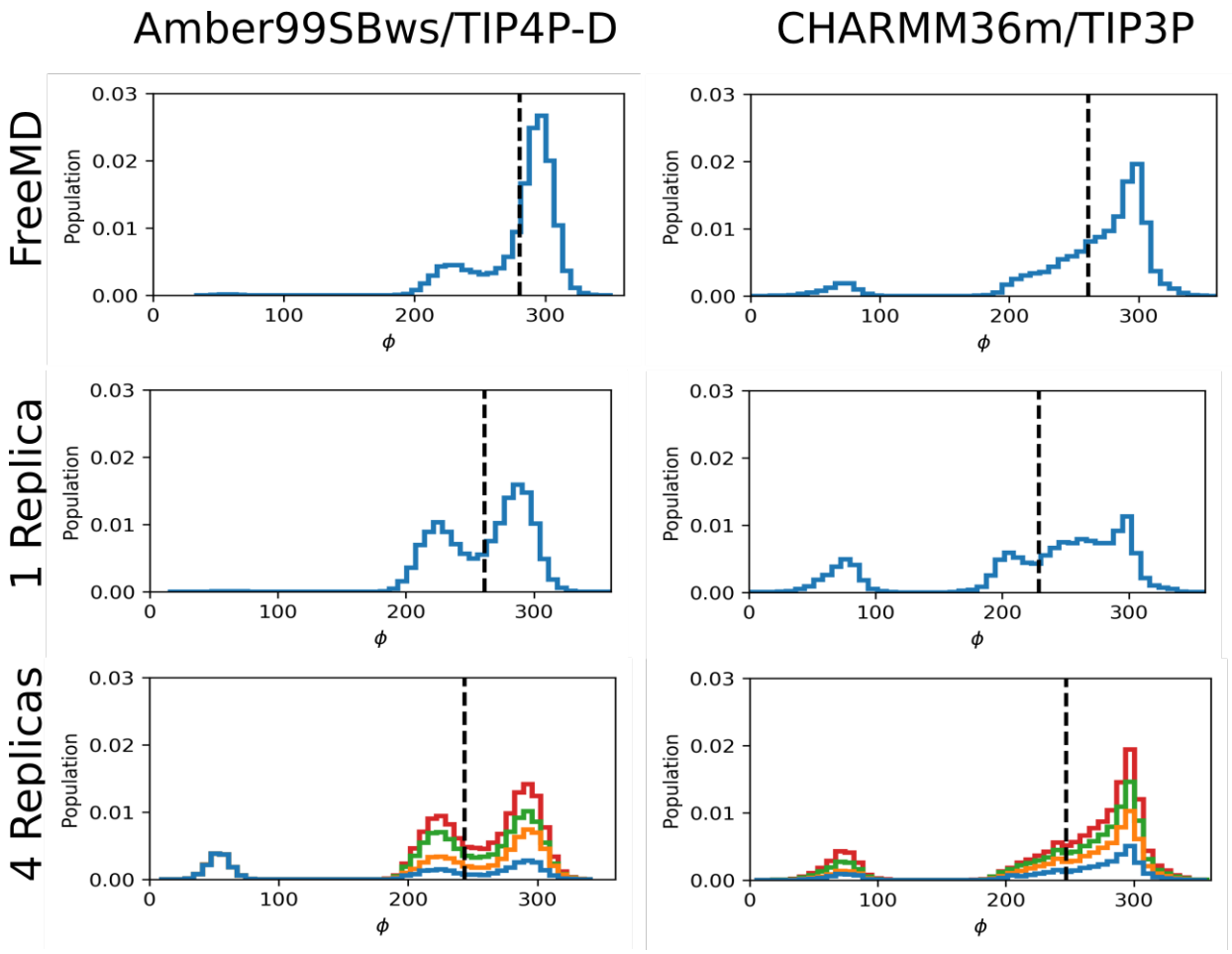

Figure S5: Distributions of the dihedral angle ϕ of residue 9 for Amber99SBws/TIP4P-D (left column) and CHARMM36m (right column). Four-replica refinement with AMBER leads to increased population of the conformations at $\phi \approx 60°$ and $\phi \approx 225°$ (left column), evidently leading to improved agreement with experimental ^3J couplings (compare with Fig. S3, shaded vertical bars and magenta lines). In contrast, the ϕ distribution of the CHARMM36m simulation was only marginally modified by the four-replica refinement (right column).